Introduction to the Proposed AISC Load and Resistance Factor Design Specification

JOHN A. EDINGER

INTRODUCTION

The proposed AISC *Load and Resistance Factor Design Specification*[1] is now undergoing a one year period of public review and comment. This culminates efforts over the past years by many individuals who have contributed significantly to the draft specification.

The intent of this paper is to provide a brief introduction to the proposed LRFD Specification by briefly discussing the basic load and resistance formulation, load and resistance factors, and providing a comparison with the present *Allowable Stress Design Specification.*[2]

LRFD FORMULATION

The limit state philosophy in design is to ensure that the combined effect of the loads does not exceed the structural resistance to particular failure modes. For example, two such limit states for a tension member are those of yielding and fracture. A limit state can also be a service limit state, such as deflection or vibration. By considering the requirements of a structure in this manner there is potential for designing safer, more efficient, and less costly structures.

The basic formulation to ensure a load effect less than the resistance is given by Eq. 1.

$$\Sigma\gamma_i Q_i \leq \phi R_n \qquad (1)$$

In this formulation, ϕ is the resistance factor prescribed in the Specification. It reflects uncertainty in the provided resistance and is always less than or equal to unity. R_n is the nominal strength of the structure and is determined in accordance with standard engineering principles. The load side of the formula consists of the load factors, γ_i, to account for potential overloads and uncertainty, and Q_i, the mean loads. The summation accounts for loads from different sources and allows for a different load factor to be assigned to each load.

The procedure involved can be demonstrated in a design example of a tension member as shown in Fig. 1.

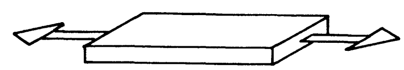

Figure 1

To determine the required area for this member subject to a dead load of two kips and a live load of five kips, we must provide a strength that exceeds the applied force. This can be represented in terms of Eq. 1 as:

$$\Sigma\gamma_i P_i \leq \phi_t R_n \qquad (2)$$

For the limit state of yielding on the gross section Eq. 2 can be written as:

$$1.2P_D + 1.6P_L \leq .90A_gF_Y$$

With a live load of five kips and a dead load of two kips and using A36 steel the result is:

$$1.2\ (2) + 1.6\ (5) \leq .90A_g(36)$$
$$10.4^k \leq 32.4\ A_g$$

Or a gross area requirement of:

$$A_g \geq 0.321\ \text{in.}^2$$

For the limit state of fracture on the effective net area Eq. 2 can be written as:

$$10.4^k \leq .75\ A_eF_u$$

$$10.4^k \leq .75\ A_e\ (58)$$

John A. Edinger is Assistant Director of Engineering, American Institute of Steel Construction, Chicago, Illinois.

Resulting in an effective net area requirement of:

$$A_e \geq 0.239 \text{ in.}^2$$

A member can then be sized to meet these requirements.

LOAD FACTORS

In the design of the structure and its elements, the appropriate combinations of loads must be considered. While this is often a matter of judgement, the proposed AISC LRFD Specification lists load combinations based upon ANSI Specification A58.1-1982[3] which represents those load combinations that are commonly encountered.

For normal loads the combinations are:

$$1.4\ D_n \tag{3}$$

$$1.2\ D_n + 1.6\ L_n + 0.5(L_r \text{ or } S_n) \tag{4}$$

where D_n is the dead load, L_n is the live load, L_r is the roof live load and S_n is the snow load. Impact loading would be included only in Eq. 4. With wind or earthquake the load combinations are:

$$1.2\ D_n + 1.6(L_r \text{ or } S_n) + (0.5\ L_n \text{ or } 0.8\ W_n) \tag{5}$$

$$1.2\ D_n + 1.3\ W_n + 0.5\ [L_n + (L_r \text{ or } S_n)] \tag{6}$$

$$1.2\ D_n + 1.5\ E_n + (0.5L_n \text{ or } 0.2\ S_n) \tag{7}$$

where W_n is wind load and E_n is earthquake load. In this instance impact loading would be included only in Eq. 5.

To account for uplift and ponding the load combinations are:

$$0.9D_n - (1.3\ W_n \text{ or } 1.5E_n) \tag{8}$$

$$1.2\ D_n + 1.2I_n \tag{9}$$

where I_n is the nominal load due to initial rainwater or ice exclusive of the ponding contribution.

RESISTANCE FACTORS

The resistance factors ϕ in the proposed LRFD Specification range from 0.60 for bearing on A307 bolts to 1.00 for bearing on pin connected members, slip resistant bolt shear values, and web yielding under concentrated loads. Table 1 lists the resistance factors and their uses.

COMPARISON WITH PRESENT SPECIFICATION

In ASD[2] the factor of safety for live load and dead load is identical. In the proposed LRFD Specification[1] the load factors will be different for live load and dead load (and other loads). Consequently, any comparison between the specifications will depend upon the live-load to dead-load ratio used to correlate them.

In building construction, the live-load to dead-load ratio varies between 0.25 and 4 (for some light structures it may be as high as 5). We know that the past performance of structures within these ranges has been satisfactory; and therefore, it is reasonable to conclude the factor of safety has been adequate. It is obvious the current factor of safety varies and, in fact, increases with a decreasing L/D ratio.

Table 1

ϕ	Application
1.00	Bearing on pin connected members Slip-resistant bolt shear values Web yielding under concentrated loads
0.90	Tension yielding Beams in bending and shear Groove welds - base metal Fillet welds - stress parallel to weld axis Local flange bending
0.85	Column Edge distance and bearing capacity at holes Web crippling and sidesway web buckling
0.80	Groove weld electrodes-tension normal to effective area
0.75	Tension fracture Pin-connected members in tension or shear Bolts in tension Partial penetration groove welds in shear Fillet weld stress on effective area Plug or slot welds
0.65	Bearing on bolts (except A307)
0.60	Bearing on A307 bolts

Low-rise structures, such as conventional commercial buildings and pre-engineered buildings, constitute a class of structures made up of a great number of steel buildings with satisfactory service records. The structures fall in the upper half of the range of L/D ratios. In view of this record of satisfactory performance, the selection of a L/D ratio of 3 is the basis for establishment of criteria at which ASD and LRFD would result in the same structure (called "calibration").

In ASD the overall factor of safety is related to:

$$\frac{D + L}{F_a} \tag{10}$$

while for the proposed LRFD Specification[1] the overall factor of safety is related to

$$\frac{1.2D + 1.6L}{\phi F_{cr}} \tag{11}$$

Setting the relationship given by (10) equal to that given by (11) we obtain:

$$\frac{D + L}{F_a} = \frac{1.2D + 1.6L}{\phi F_{cr}} \tag{12}$$

or

$$\frac{\phi F_{cr}}{F_a} = \frac{1.2 + 1.6\ (L/D)}{1 + L/D} \tag{13}$$

Substituting into Eq. 13 a L/D ratio equal to 3 results in;

$$\frac{\phi F_{cr}}{F_a} = \frac{6}{4} = 1.5$$

or

$$\phi F_{cr} = 1.5\ F_a \tag{14}$$

That is, the LRFD design strength equals 1.5 times the present allowable strength.

For tension members, the weight is directly proportional to required strength. It follows then that the weight of the LRFD member relative to the weight of the ASD member is given by combining Eq. 12 with Eq. 14.

$$W_{LRFD}/W_{ASD} = \frac{1.2 + 1.6(L/D)}{1.5\ (1 + L/D)}$$

This relationship is shown in Fig. 2

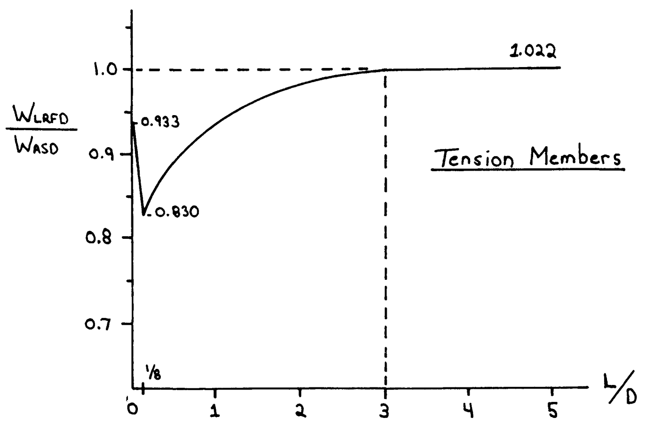

Figure 2

In Fig. 2, the relative weight is given as a function of the live- to dead-load ratio. LRFD shows weight savings when this ratio is less than three. When the live- to dead-load ratio is less than 1/8, the relationship is no longer valid because the member designed by LRFD is then governed by the dead-load only load combination of 1.4D (Eq. 3). As a result a separate curve is shown in Fig. 2 for live- to dead-load ratios in the range from 0 to 1/8.

The maximum weight savings for a tension member is 17% at a live-load to dead-load ratio of 1/8. Correspondingly, the maximum weight increase at an upper limit of live-load to dead-load ratio of five is only 2.2%.

A similar analysis can be made for beams and girders. For the economy series of wide flange beams, the weight is proportional to the 2/3 power of the required bending strength[4]. Fig. 3 shows the resulting weight of the LRFD member relative to the ASD member.

Again, the maximum weight savings of 11.5% is considerable, whereas the maximum weight increase is 1.5% at a live-load to dead-load ratio of five.

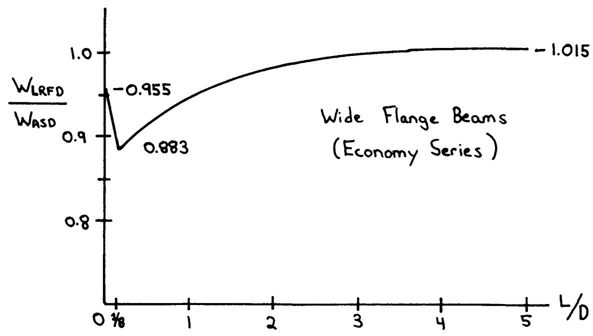

Figure 3

Some controversy still exists regarding the column formula that should be used for LRFD. In the present proposed AISC LRFD Specification[1] the existing ASD[2] formula has been reformated in LRFD terms.

Recalling from Eq. 14 that for a live-load to dead-load ratio of three:

$$\phi F_{cr} = 1.5 F_a \tag{14}$$

From Table 1 the resistance factor ϕ for columns is 0.85 and Eq. 14 can be written as:

$$F_{cr} = 1.76 F_a \tag{15}$$

Therefore, the new stress for columns designed in accordance with the proposed LRFD Specification will be 1.76 times the present allowable values. For a given length, the weight savings using LRFD as a function of the live-load to dead-load ratio is the same as for tension members, shown in Fig. 4.

It must be stressed that this is an interim solution. In the last two decades a great deal has been learned about the strength of actual columns and actually this knowledge should be incorporated into any new specification.

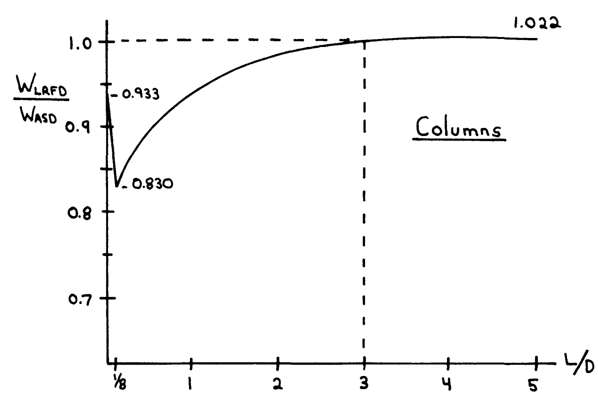

Figure 4

SUMMARY

The proposed AISC LRFD Specification is currently out for a year of public review and comment. After this, public reaction will be considered, and a final version of the LRFD Specification presented to the AISC board of directors.

It is hoped this brief description of the proposed AISC *Load and Resistance Factor Design Specification* will serve as an adequate introduction to the proposed specification.

In any event, the main conclusion is that the reason for adopting LRFD is not the achievement of immediate economical advantages, but the opportunities for future advancement in the state of the art of steel design.

REFERENCES

1. *American Institute of Steel Construction* Proposed AISC Load and Resistance Factor Design Specification *Chicago, Ill., April 15, 1983.*
2. *American Institute of Steel Construction* Specification for the Design, Fabrication and Erection of Structural Steel for Buildings (effective Nov. 1, 1978) *Chicago, Ill.*
3. *American National Standards Institute, Inc.* Minimum Design Loads for Buildings and Other Structures, ANSI A58.1-1982 *New York, N.Y.*
4. *Haaijer, G.* Economy of High Strength Steel Structural Members *Trans. ASCE, Vol. 2, 1963 (p. 820).*

loads. The braced frame and framed tube exhibit different deformation patterns when subjected separately to lateral loads. A framed tube deforms predominately in a shear mode (Fig. 6a). On the other hand, a braced frame deforms primarily in bending mode (Fig. 6b). When both elements are connected by floor slabs, normally considered rigid in their own planes, identical displacement is enforced. The interaction between the two elements is such that the frame reduces the lateral deflection of the braced frame at the top. But near the base of the structure, the braced frame tends to dominate the deformed configuration. Interaction forces resulting from the different deformation patterns are shown in Fig. 6c. Obviously, the distribution of the applied shear to the resisting element in proportion to their relative stiffnesses can lead to erroneous results.

A typical variation of the interaction forces is shown in Fig. 6d for an applied static earthquake direction along the plane of the braced frame. The interaction forces are expressed as a ratio of the shear force as carried by the braced frame to that of the applied shear at the building height under consideration. It is important to note that at top stories, the total shear carried by the frame can exceed the applied story shear. This condition is evident from the observation of the shear forces in the braced frame, which act in the same direction as the applied loads. Fig. 6d also shows the increase in horizontal shear in the braced frame at the lower stories, where the braced frame is relatively stiffer than the framed tube. During a major earthquake, the yielding of the frame tube columns will impose additional strength requirements in the braced frame. The character of shear distribution, as discussed, is typical of a dual system.

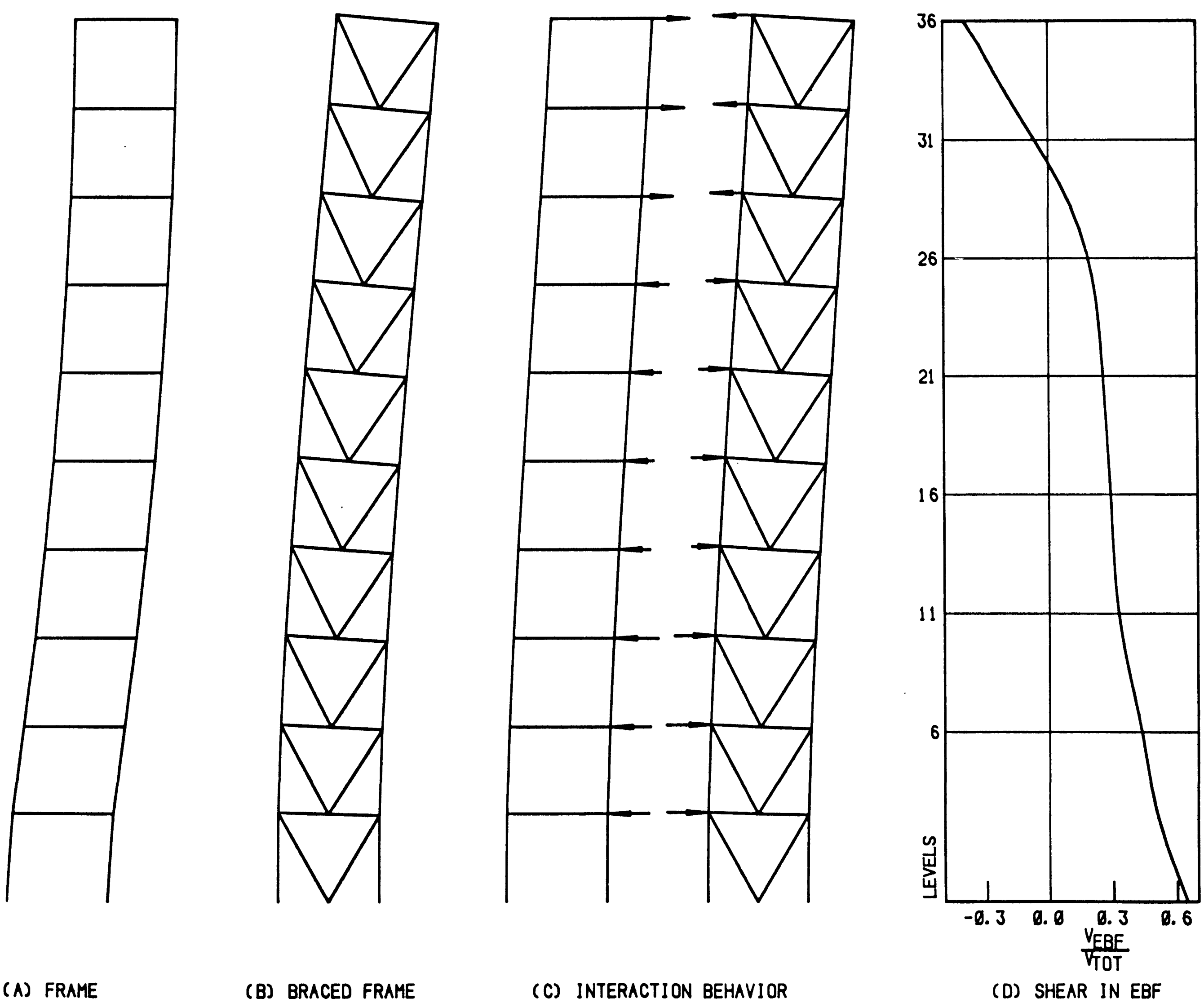

Fig. 6. Frame-braced frame interaction

Seismic Application of Dual System—Current building codes'[8,9] provisions have discouraged the application of dual systems in seismic zones. In conventional dual system (K = 0.8), where a concentrically braced frame (CBF) is used, from experimental studies[19] it was found that CBF exhibits pinched and deteriorating hysteretic behavior as a result of buckling of the brace under repeated and reversed loading. This indicates poor energy dissipation capability as well as stiffness degradation. Such behavior can be eliminated if the braced frame remains elastic during severe earthquake excitation. Present codes[8,9] stipulate that 100% of the total base shear is to be resisted by the braced frames, for the purpose of substituting elastic behavior for ductility demands. In high-rise buildings, this criterion cannot be easily satisified, primarily because the stiffness contribution of the braced frame is comparable, or in some cases, smaller than that of the moment frames (see Fig. 6d). The foregoing criterion will generally require members of large proportion as well as an additional cost premium to the project. From these considerations, a dual system with CBF is seldom used.

On the other hand, experimental studies[2] on EBF confirm the favorable energy dissipation and stiffness behavior during cyclic tests. Such behavior is essential to the satisfactory performance of a structure during a severe earthquake. Recognizing the ductile behavior of the EBF, the requirement that the braced frame resist 100% of the base shear was waived by the building authority for this project. Therefore, in seismic regions, the EBF would be preferred over a CBF in a dual system.

PLANNING REQUIREMENTS OF ECCENTRICALLY BRACED FRAMES (EBF)

The design procedures and behavior of an EBF have been well-documented.[16,17] Planning requirements and functional considerations during design phase will be considered here.

To minimize interference with architectural functions, the EBF can be located ideally between adjacent elevator cores. Due to the wide spacing between columns, and also

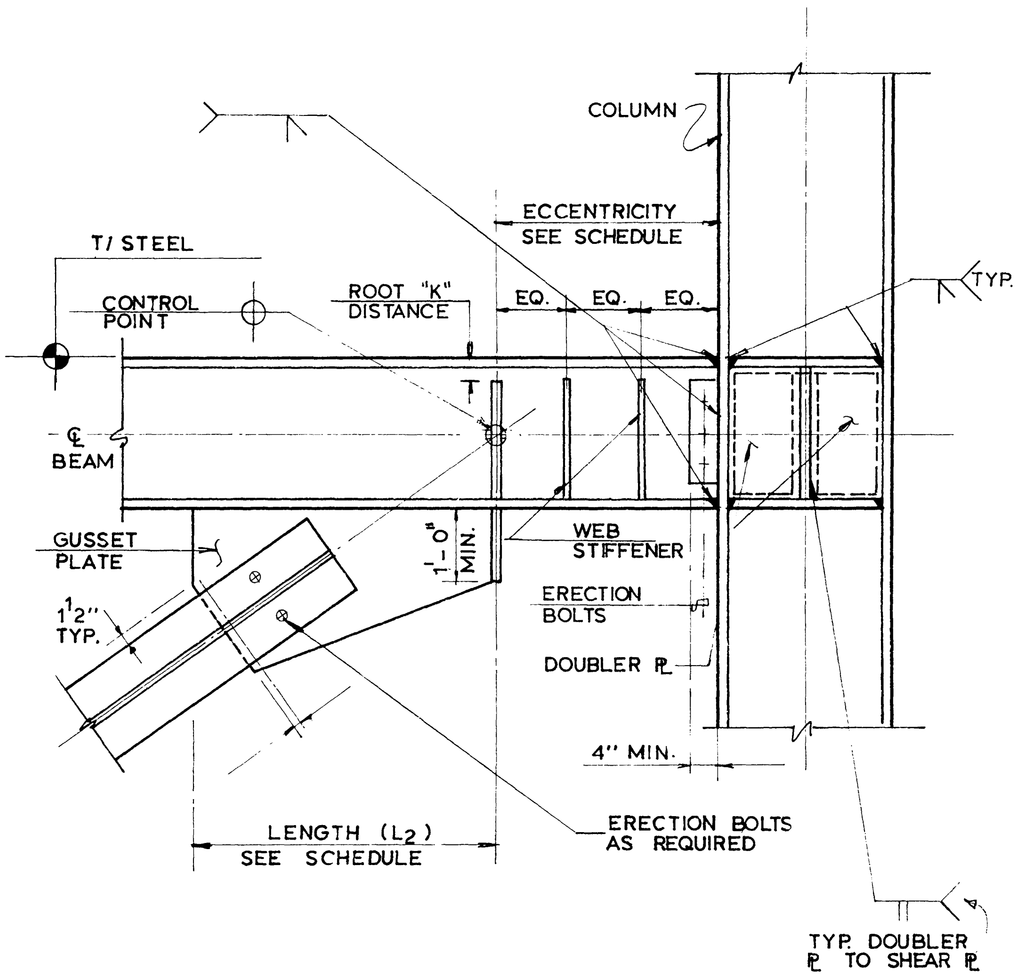

Fig. 7. Eccentrically braced frame detail at column end

for accessibility purposes, the inverted K configuration is used. Active shear links (Fig. 7) are provided at both ends of the beam adjacent to the column. It is important to note that the active shear link has to be braced at the work point of the beam—brace intersection, to inhibit lateral torsional buckling under large deformations. However, such beam braces cannot be accommodated without interfering with the elevator operations. During the early development phase of the project, coordination with the architect warranted a layout of the elevators to allow for the beam brace. The brace elements are comprised of two WT sections laced together with intermediate spacer plates to form an integral unit. The active link beam elements are designed to withstand the stress induced by the maximum probable earthquake (to be defined later) according to the interaction formula:

$$f_a/F_a + f_b/F_b = 1.0 \qquad (2)$$

in which f_a is the computed axial stress resulting from the horizontal components of the brace forces. The eccentricity in the brace offset is proportioned to insure shear yielding in the beam elements such that :

$$Vp = 2.0{*}M_p/L \qquad (3)$$

Due to the large magnitude of earthquake forces, the beam members used in the project range from W27 to W36's, which far exceed the test specimens as reported by Roeder and Popov in the previous test. To insure the stability of the beam web during inelastic yielding, additional web stiffeners were added. Upon Popov's recommendation, web stiffeners were spaced such that:

$$S/t \leq 30 \qquad (4)$$

where S is the spacing of stiffeners and t is the web thickness.

His recommendation is based on recent research findings on tests of wide flange sections of 18 in. and larger depth. Typical details of EBF connections at mid-span and active link ends at the column are shown in Figs. 7 and 8.

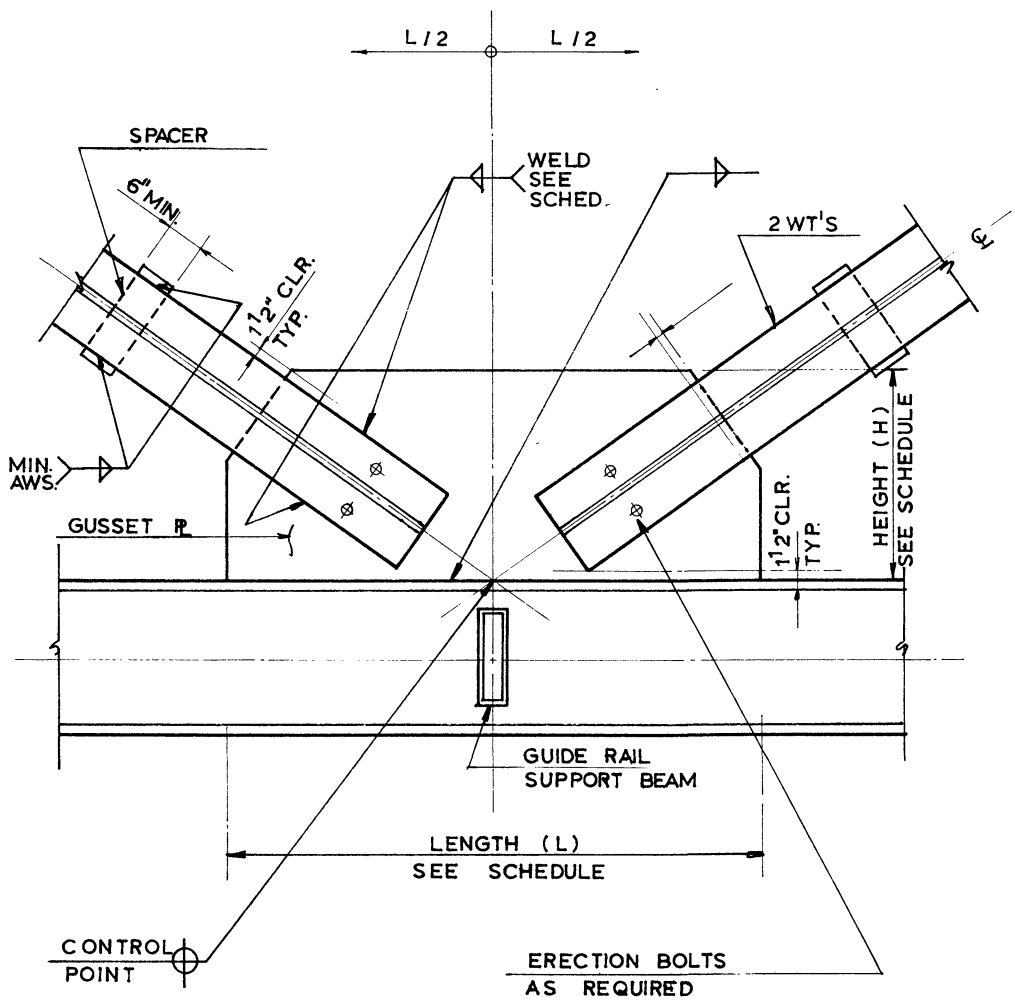

Fig. 8. Eccentrically braced frame detail at mid-point

DYNAMIC ANALYSES

Performance of a complex structure during earthquake excitation cannot be accurately predicated by the code prescribed "Equivalent Static Earthquake" approach. For a building with a complex structural system and shape such as the Getty Plaza, a detailed dynamic analysis is warranted. Linear elastic dynamic analysis employing the response spectrum method was carried out with a three-dimensional mathematical model using the program ETABS.[10]

For dynamic analysis, the seismic design criteria as set forth by the Los Angeles City Building Department[11] require that the structure meet two different levels of earthquake performance, based on the magnitude of two different earthquake events. First, for the maximum probable earthquake, defined as an event with 50% probability of being exceeded in a 50-year period, the structure has to remain essentially elastic. Second, from the considerations of the local geological conditions, the most extreme earthquake that can be anticipated, defined as the maximum credible earthquake, the structure shall not collapse, and controlled inelastic action is anticipated. Seismic studies were undertaken to determine the magnitude of such events. Fig. 9 shows the response spectra[13] with proper modification for the regional and local site conditions.

Of great importance in dynamic analysis are the structural stiffness properties. The contribution of the panel zone stiffness in a framed-tube structure will be reviewed in this section. Furthermore, problems associated with the unusual geometry of the example building will be examined.

Stiffness Formulations—The dynamic properties of the structure are directly related to the overall building stiffness. For a framed-tube structure, the finite member joint size (panel zone) has a significant contribution to the overall building stiffness, and therefore directly affects the building response to earthquake excitation. If rigid behavior of the panel zone is assumed, then the stiffness of the frame will be overestimated. The story deflection resulting from the panel zone deformation d_{zone} can be calculated approximately from the portal method. This assumes that points of

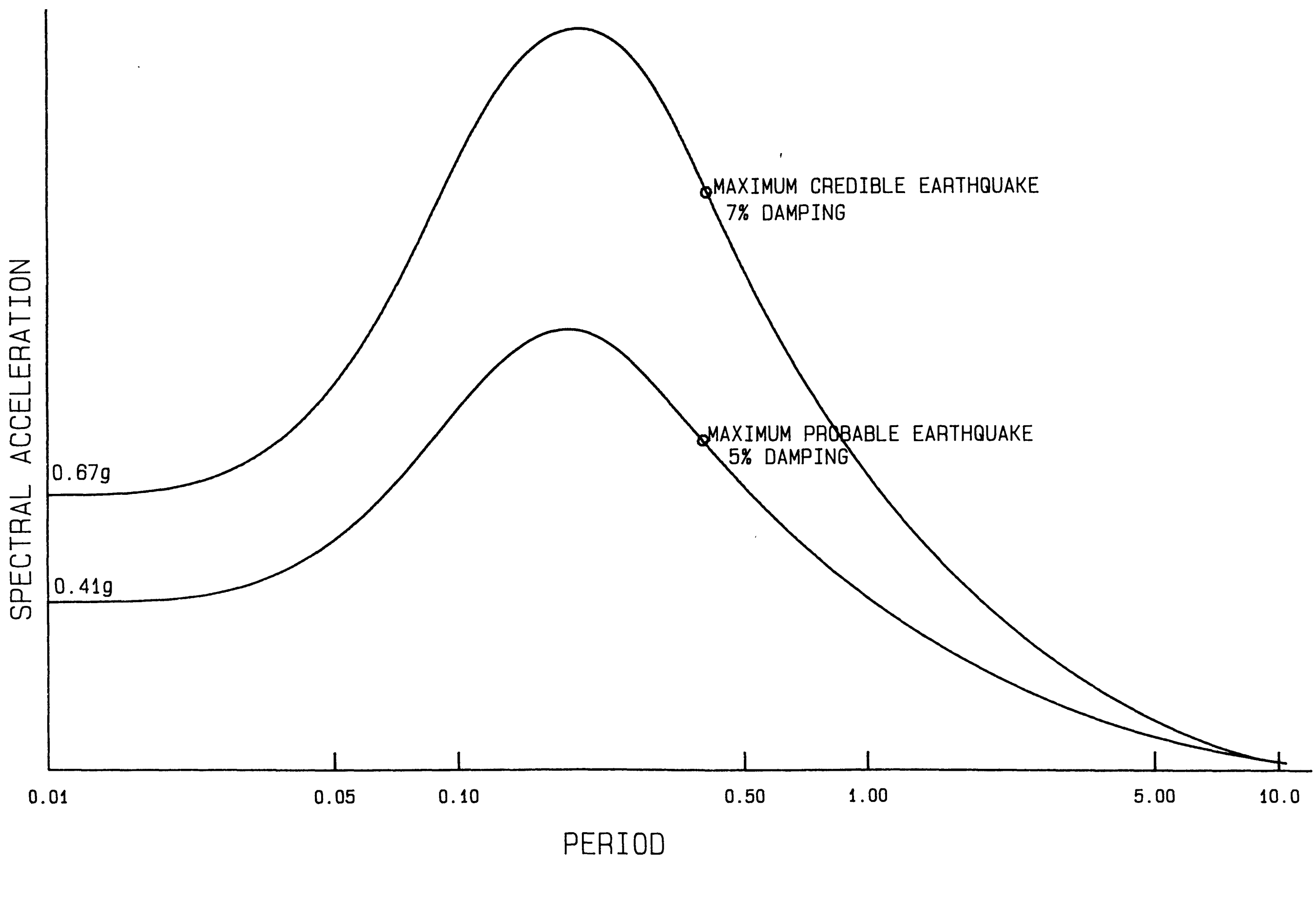

Fig. 9. Response spectra

inflection occur at mid-heights of columns and at mid-spans of beams. Krawinkler[12] reports such deflection under unit lateral load to be:

$$d_{zone} = \frac{h - d_b}{d_c t G} \tag{5}$$

where d_b,d_c are the finite beam and column depths, t is the web thickness, including doubler plate if any, H is the story height and G is the shear modulus.

It is common practice to represent the mathematical model based on the center line dimensions of the physical structure, in which case, the stiffness of the panel zone should be modelled with appropriate methods.

Critical Directions of Earthquake—Once the stiffness and mass properties of the structure are defined, the mode shapes and frequencies can be determined from the classical free vibration problem. The periods, as well as the directions of the mode shapes, are shown in Table 1 and in Fig. 10 for this example building. Figure 11 shows the configurations

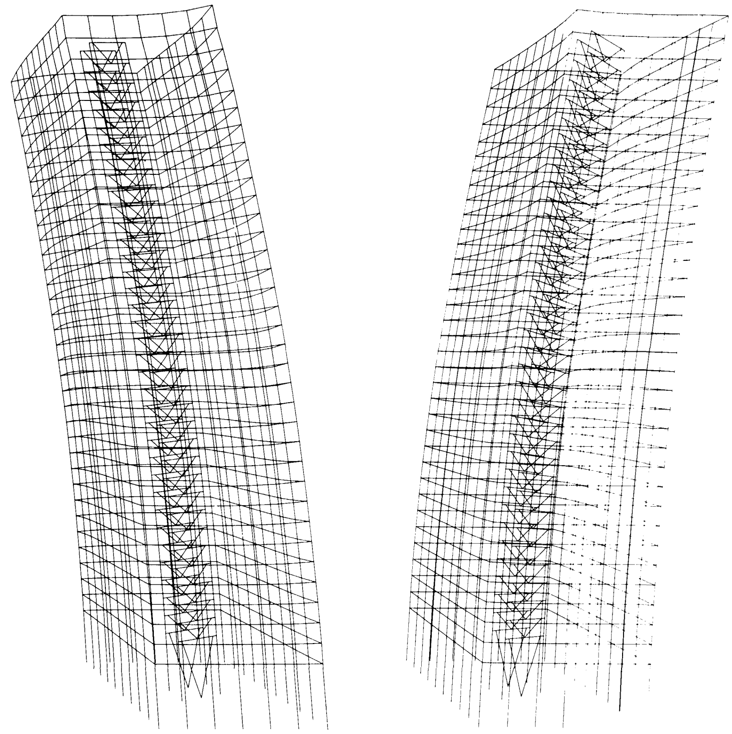

Fig. 11. Principal translation mode shape configuration

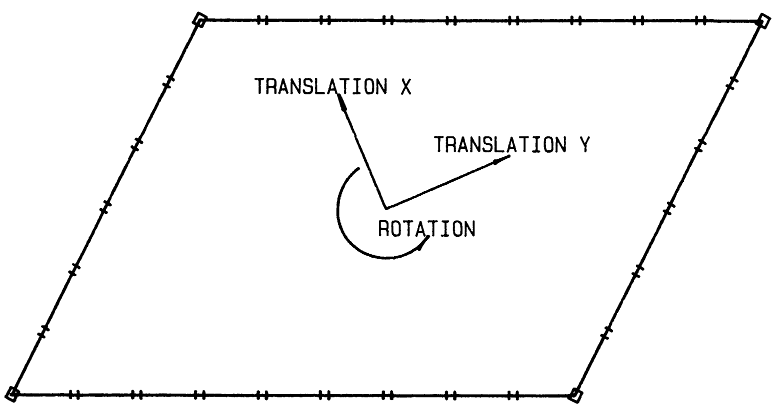

DIRECT-ION / MODES	TRANSLATION X	TRANSLATION Y	ROTATION θ
1st Mode	4.900	3.240	2.585
2nd Mode	1.880	1.396	1.180
3rd Mode	1.071	0.869	0.758
4th Mode	0.709	0.592	0.523
5th Mode	0.524	0.460	0.400
6th Mode	0.408	0.379	0.326

Fig. 10. Directions of fundamental mode shapes and building period

Table 1

Responses / Components	Responses in X & Y			Critical Directions		
	X	Y	$\Sigma f_{xi} f_{yi}$	P $\theta_{cr} = -69.4°$	M_x $\theta_{cr} = 23.1°$	M_y $\theta_{cr} = 22.9°$
P Kips	939.0	2013.0	−1384604	2138.2	608.7	607.6
M_x ft-kips	914.4	590.4	254442	491.3	972.0	972.0
M_y ft-kips	562.0	311.8	112409	224.2	602.7	602.8

of the two principal fundamental translation modes. In the response spectrum method of analysis, the response of an individual mode to a particular earthquake motion can be obtained from the spectral values of a single degree of freedom system (Fig. 9). In view of the fact these individual maximum modal responses do not occur at the same time, a better estimate of the maximum overall system response is obtained from statistical combination of the modal maxima. Different combination methods[14,18] have been proposed, of which the square root of the sum of the squares combination has particular interest. In this method, the overall response is expressed as:

$$f_{max} = \sqrt{\Sigma f^2_i} \tag{6}$$

where f_{max} denotes the estimated maximum response and f_i is the modal maximum of the ith mode.

In most cases, a simplification of the true three-dimensional earthquake response of structure is made by assuming the design horizontal acceleration components to act non-concurrently in the direction of the main axes of a building. It is generally accepted that a building designed by this approach will have adequate resistance against the acceleration acting in any direction. However, it is doubtful such assumption is valid for this example structure. In particular, the main axes of this building are not well defined. As clearly illustrated in Fig. 10, the alignments of the mode shape axes are skewed with respect to the planes of the frames. Therefore, the critical directions of earthquake must be quantitatively evaluated to determine what will produce maximum forces and deformations.

Consider a three dimensional structure, subjected to earthquake excitation along two arbitrary horizontal axes X and Y, which are mutually perpendicular to each other. The modal responses, as well as the overall response, can be readily calculated along each axis. For an earthquake excitation along an axis, inclined at an angle θ to the x axis, the overall response (F_θ) can be represented as:

$$F_\theta = \sqrt{(f_{xi}\cos\theta + f_{yi}\sin\theta)^2} \tag{7}$$

where f_{xi}, f_{yi} denotes the responses along the X and Y axes respectively for the ith mode.

This equation can be simplified as:

$$f_\theta = \sqrt{F_x^2\cos^2\theta + F_y^2\sin^2\theta + \sin 2\theta\Sigma f_{xi}f_{yi}} \tag{8}$$

where F_x,F_y represents the overall response along the X and Y axis.

The critical angle (θ_{cr}) for maximum response can be then obtained by:

$$\frac{d(F_\theta)}{d\theta} = 0.0 \tag{9}$$

thus, the critical angle can be shown to be:

$$\tan(2\theta, 180+2\theta) = \frac{2\Sigma f_{xi}f_{yi}}{F_x^2 - F_y^2} \quad \text{where } 90 \geq \theta \geq -90 \tag{10}$$

These formulations can be readily incorporated into existing analysis programs, and enable the calculations of critical angles from the responses along two orthogonal axes. As can be seen from Equation 10, for a column member, the critical angles for axial force, major and minor axis bending moments can have different values. However in the design of this member in accordance with the interaction formulas of the AISC Specification,[15] these variables are evaluated along the same angle of earthquake input. Table I shows the critical angles for a typical corner frame column. This column is of rectangular shape box section. In this particular case the critical angles for the major and minor axis bending are essentially identical and the critical angle for maximum axial load is along one of the principal mode shape directions.

The foundation system for the perimeter-tube structure consists of a continuous strip footing, with depth varying from six to eight ft. This footing is analysed as a beam on an elastic grade. Since the equations previously developed are valid only for individual members, for a continuum such as the strip footing, the corresponding forces and bending moments on all columns resulting from the same direction of earthquake excitation have to be evaluated globally. Five earthquake directions are examined along the following directions: (a) the principal mode shape directions (3 directions) (b) the direction along the plane of each frame (2 directions). The earthquake along the direction of the braced frames was found to produce the maximum bearing pressure underneath the footing for this structure.

CONCLUSIONS

In the design of building structures located in areas of high seismic risk, the proper balance between stiffness and ductility must be maintained. The dual system, as used in Getty Plaza Tower, fulfills both of these objectives. With proper detailing both of the components in this system, the perimeter framed tube and the interior EBF, exhibit excellent energy dissipation capability, essential to the satisfactory performance of the building during a major earthquake. In addition, the advantages of this system in meeting the stiffness requirements at relatively low cost provide an economical solution for highrise framing.

Due to the non-ductile behavior of CBF, current building codes stipulate the braced frame component in a dual system has to be designed for the total seismic base shear. In contrast, the EBF demonstrates excellent energy dissipation capability. This code requirement should be revised to recognize such behavior, and to establish proper classification for such systems in a seismic application.

The deflection and dynamic characteristics of the Getty Plaza Tower have been identified. To a large extent this behavior is typical for buildings with general configurations. For such general shaped structures the prediction of the critical angles of earthquake excitations that produces the maximum force or deformation in a particular member is not readily apparent. Formulations are presented which enable the calculations of such angles from the responses of two orthogonal earthquake directions.

To provide an economical framing system for the Getty Plaza Tower, a unique dual structural system was developed. The unusual configuration of the structure required close examination of its stiffness and dynamic properties, and led to a better understanding of the general behavior of a three-dimensional structure.

ACKNOWLEDGEMENTS

The Getty Plaza project is jointly developed by MCA Inc. and Getty Oil Co. The writer is indebted to the late Fazlur R. Khan for his encouragement of the use of the system. The review of the eccentrically braced frame details by Egor P. Popov is gratefully acknowledged. Gratitude is also expressed to Lauren Carpenter, project engineer, and Francis Lau for their valuable suggestions for this paper.

NOMENCLATURE

f_a = computed axial stress
F_a = allowable axial stress
f_b = computed bending stress
F_b = allowable bending stress
F_x, F_y = axial or bending stress
G = shear modulus
h = story height
K = system factor for equivalent static earthquake method
L = span for beam
M_p = plastic moment capacity
V_p = modified yield shear capacity
X,Y = principal directions of mode shapes

REFERENCES

1. *Iyengar, S. H.* Preliminary Design and Optimization of Steel Building Systems *State of Art report, Proceedings of the International Conference on Planning and Design of Tall Buildings, ASCE and IABSE, 1972.*
2. *Roeder, C. W. and E. P. Popov* Inelastic Behaviour of Eccentrically Braced Steel Frames under Cyclic Loadings *Report No. EERC 77-18, Earthquake Engineering Research Center, University of California, Berkeley, Cal., August 1977.*
3. *Libby, J. R.* Eccentrically Braced Frames Construction—A Case Study *AISC Engineering Journal, 4th Qtr., 1981, Chicago, Ill.*
4. *Merovich, A. T. et al* Eccentric Bracing in Tall Buildings *Journal of Structural Division, ASCE, Vol. 108, ST9, September 1982.*
5. *Wong, C. H. et al* Preliminary Design and Member Sizing of Tall Steel Buildings *AISC Engineering Journal, 2nd Qtr., 1981, Chicago, Ill.*
6. *Kahn, F. R. and N. Amin* Analysis and Design of Framed Tube Structure for Tall Concrete Buildings *American Concrete Institute Publication SP-36, Response of Multistory Structures to Lateral Forces.*
7. *Khan, F. R. and J. A. Sbarounis* Interaction of Shear Wall and Frames *Journal of Structural Division, ASCE, Vol. 90 ST3, June 1964.*
8. Uniform Building Code *International Conference of Building Officials, 1978 Edition, Whittier, Cal., 1978.*
9. City of Los Angeles Building Code *City of Los Angeles Building and Safety Department, 1980.*
10. *Wilson, E. L. et al* Three Dimensional Analysis of Building Systems (Extended version) *Report No. EERC 75-13, Earthquake Engineering Research Center, University of California, Berkeley, 1975.*
11. *Harder, R.* L. A. City—Dynamic Analysis *Symposium by Structural Engineer Association of Southern California, March 1978.*
12. *Krawinkler H.* Shear in Beam-Column Joints in Seismic Design of Steel Frames *AISC Engineering Journal, 3rd Qtr., 1978, Chicago, Ill.*
13. *Woodward-Clyde Consultants* Geotechnical Investigation—Getty Plaza, Universal City, California *May 1982.*
14. *Applied Technology Council* ATC-2, An Evaluation of a Response Spectrum Approach to Seismic Design of Buildings *September 1974.*
15. *American Institute of Steel Construction* Manual of Steel Construction *8th Ed., Chicago, Ill., 1980.*
16. *Teal, E. J.* Practical Design of Eccentric Braced Frames to Resist Seismic Forces *Structural Steel Educational Council, 1979.*
17. *Roeder, C. W. and E. P. Popov* Eccentrically Braced Steel Frames for Earthquakes *Journal of Structural Division, ASCE, Vol. 104, No. ST3, March 1978.*
18. *Wilson, E. L. et al* A Replacement for the SRSS Method in Seismic Analysis *Earthquake Engineering and Structural Dynamics, Vol. 9, 1981.*
19. *Wakabayashi, et al* Experiment on the Elastic-Plastic Behavior of Bars Subjected to Cyclic Axial Loads *Reprints of Annual Conference, AIJ, October 1972.*